This is a repository copy of *An optimal finite element mesh for elastostatic structural analysis problems*.

Article:

White Rose Consortium ePrints Repository

http://eprints.whiterose.ac.uk/

This is an author produced version of a paper published in **Computers and Structures.**

White Rose Repository URL for this paper:
http://eprints.whiterose.ac.uk/1661/

Published paper
Jimack, P.K. (1997) *An optimal finite element mesh for elastostatic structural analysis problems.* Computers and Structures, 64 (1-4). pp. 197-208.

An Optimal Finite Element Mesh for Elastostatic Structural Analysis Problems

P.K. Jimack
School of Computer Studies
University of Leeds
Leeds LS2 9JT, UK

Abstract

This paper investigates the adaptive solution of a class of elastic structural analysis problems through re-positioning of the finite element nodal points (*r*-refinement) using an approach known as the Moving Finite Element method. Initially this adaptive method is derived for the elasticity problems of interest and it is then proved that, under certain conditions, the algorithm can yield optimal piecewise linear solutions on optimal simplicial finite element meshes. The equations of linear elasticity are then used to illustrate both the method itself and the optimality result that is derived. Finally, a number of numerical calculations are made to provide verification of the theoretical results.

1 Introduction

The problem of attempting to find an optimal finite element mesh for performing structural analysis has been considered by numerous authors over the past 20 years or so (see [5], [7], [8] or [21] for example). Many possible approaches have been considered, including methods based on energy minimization (such as [7]) and others based upon geometric considerations (such as [5]). In addition numerous different remeshing techniques have also been considered, based upon either *h*-refinement ([23]), where extra mesh points are added locally, or *r*-refinement ([5]), where a fixed number of mesh points are redistributed over the computational domain. Other forms of adaptive analysis have also been considered, such as *p*-refinement for example (where the degree of the finite element approximation is allowed to increase to obtain higher accuracy, [4]), or various combinations of these. In all cases however the general aim is to improve the quality of the finite element approximation space so as to allow accurate solutions to be reliably found at the lowest possibly computational expense.

In this paper we consider a remeshing technique based upon the use of *r*-refinement, with a fixed number of degrees of freedom. The approach that we follow is slightly different to most of the papers cited above since this work is motivated primarily by an analysis ([10], [11]) of a finite element technique that was originally intended for use with transient problems, known as the Moving Finite Element method, due to Miller *et al* ([9], [16] and [17]). This method has been applied to a wide variety of time-dependent problems of both hyperbolic (e.g. [2]) and parabolic (e.g. [14]) nature. The idea behind it, which is explained in more detail in section 2 below, is to produce a finite element scheme in which the mesh deforms continuously with time as the solution evolves. In this work, we obtain solutions to elastostatic structural analysis problems through the use of artificial time-stepping in such a way that the final solution obtained turns out to be an optimal finite element solution on an optimal mesh.

7

A general form of the elastostatic problem in structural analysis is to attempt to find the displacement $\underline{u}(\underline{x})$ which minimizes the total stored energy of a body initially occupying a domain $\Omega \subset \Re^D$:

$$\min_{\underline{u}:\Omega\to\Re^D} \int_\Omega F(\underline{x}, \underline{u}, \nabla\underline{u}) \, d\underline{x} \, , \tag{1.1}$$

where $F : \Re^D \times \Re^D \times \Re^{D\times D} \to \Re^+$ is an appropriate energy density function. Depending upon the nature of the problem there may also be a boundary integral present in the functional (1.1) to represent the effects of possible traction boundary conditions for example. For simplicity however we will not consider such additional terms for the time-being.

When the displacement field $\underline{u}(\underline{x})$ is small it is common to consider the linear elasticity problem obtained by choosing

$$F(\underline{x}, \underline{u}, \nabla\underline{u}) = \frac{1}{2}\frac{\partial u_i}{\partial x_j}C_{ijk\ell}\frac{\partial u_k}{\partial x_\ell} - \rho b_i u_i \, , \tag{1.2}$$

where $\rho(\underline{x})$ is the mass density, $\underline{b}(\underline{x})$ is an external body force, $C_{ijk\ell}(\underline{x})$ are the components of a fourth order elasticity tensor, and the usual summation convention has been employed over repeated suffices. It will be assumed that the elasticity tensor is positive and has the symmetries

$$C_{ijk\ell} = C_{k\ell ij} = C_{jik\ell} = C_{ij\ell k} \, , \tag{1.3}$$

and that $\underline{u}$ satisfies displacement boundary conditions of the form

$$\underline{u} = \underline{d} \quad \text{on } \partial\Omega. \tag{1.4}$$

(In fact the generalization of what follows to take account of traction boundary conditions is quite straightforward and will be considered at the end of the paper.)

In the next section of the paper we introduce the Moving Finite Element method and show how it can be applied to the elastostatic problem (1.1) with the aid of an artificial time parameter τ. The specific choice of F given by (1.2) is also highlighted. In section 3 it is then proved that the r-refinement that is induced by this approach can lead to an optimal minimizer of the functional in (1.1) over all variations in the finite element mesh as well as variations in the nodal displacement values. That is, the Moving Finite Element method can yield an optimal mesh for the solution of this class of problem. Again, the linear problem (1.2) is considered as a specific example and it is shown that this result implies that the error in the displacement is minimized when measured in the corresponding energy norm. Finally, in section 4 a couple of simple example problems are solved numerically so as to verify the analytic results. The extension to a wider class of boundary conditions is also demonstrated and there is a brief discussion of the applicability of this work. Throughout the paper we only consider the case $D = 2$ (two-dimensional elasticity problems). In theory however all of the work can be extended to three-dimensional problems.

2   The Moving Finite Element Method

Returning now to the functional in (1.1), it can easily be seen that any minimizer, $\underline{u} : \Omega \to \Re^2$, is a solution of the Euler-Lagrange equations

$$-F_{,2i}(\underline{x}, \underline{u}, \nabla\underline{u}) + \frac{d}{dx_j}F_{,3ij}(\underline{x}, \underline{u}, \nabla\underline{u}) = 0 \tag{2.1}$$

for $i = 1, 2$, where $F_{,k}(\cdot, \cdot, \cdot)$ represents differentiation of F with respect to its kth dependent variable and the other suffices represent tensor components in the usual manner (with summation always implied over repeated suffices). As outlined in section 1 we now introduce an artificial time parameter,

τ, and consider solving the parabolic problem

$$\frac{\partial u_i}{\partial \tau} = -F_{,2i}(\underline{x}, \underline{u}, \nabla \underline{u}) + \frac{d}{dx_j} F_{,3ij}(\underline{x}, \underline{u}, \nabla \underline{u}) \tag{2.2}$$

on a continuously deforming spatial mesh. Any steady solution of this new problem will clearly also be a solution of (2.1) and so a minimizer in (1.1).

In subsection 2.1 we show how the Moving Finite Element method is derived for solving the problem (2.2) on a moving mesh. Note that in practice the steady solution of this problem will be determined by taking a finite number of "time"-steps and so the solution process is not actually that different from a more conventional adaptive strategy involving numerous solution/remeshing iterations (although the underlying philosophy is indeed rather different). The shorter subsection 2.2 which follows then illustrates the method by considering the linear problem given by (1.2), as originally outlined in [12].

2.1   Applying the MFE Method

We wish to obtain a steady solution $\underline{u}$ of the parabolic problem

$$\frac{\partial u_i}{\partial \tau} = -F_{,2i}(\underline{x}, \underline{u}, \nabla \underline{u}) + \frac{d}{dx_j} F_{,3ij}(\underline{x}, \underline{u}, \nabla \underline{u}) \quad (i = 1, 2) \tag{2.3}$$

on the domain Ω, subject to displacement boundary conditions of the form (1.4). To simplify the algebra that follows it will be convenient to assume that $\underline{d} \equiv \underline{0}$ and that Ω is polygonal. It will also be helpful to introduce the following notation. Let Ω be discretized into a set of non-overlapping triangles which can be uniquely specified as a mesh $\mathcal{M} = (\underline{s}, \mathcal{C})$, where

$$\underline{s} = (\underline{s}_1, ..., \underline{s}_N, \underline{s}_{N+1}, ..., \underline{s}_{N+B}) \tag{2.4}$$

is an ordered set of the position vectors of the vertices of the mesh (N interior points and B points on the boundary), and $\mathcal{C}$ is a list of all of the edges. The MFE method seeks to approximate $\underline{u}(\underline{x}, \tau)$, the solution of (2.3), by a time-dependent piecewise linear function, $\underline{u}^h$ say, defined on a mesh of triangles $\mathcal{M}(\tau) = (\underline{s}(\tau), \mathcal{C})$ covering the spatial domain Ω. As has been indicated, this mesh is allowed to deform smoothly in time (in what follows we always refer to the dependent variable τ as "time") by allowing the positions of the internal knot points, $\underline{s}_1(\tau), ..., \underline{s}_N(\tau)$, to be time-dependent. Their connectivity $\mathcal{C}$ remains fixed however.

Because $\mathcal{C}$ is kept fixed throughout we will generally refer to a mesh $\mathcal{M}(\tau) = (\underline{s}(\tau), \mathcal{C})$ only by the ordered set $\underline{s}(\tau)$ for notational convenience. Given that this is the case we can write our piecewise linear approximation, $u_i^h(\underline{x}, \tau)$, to each component $u_i(\underline{x}, \tau)$ of the true solution as

$$u_i^h(\underline{x}, \tau) = \sum_{m=1}^{N} a_{mi}(\tau) \alpha_m(\underline{x}, \underline{s}(\tau)) , \tag{2.5}$$

where the α_m's are the usual continuous piecewise linear "hat" basis functions on the mesh $\underline{s}(\tau)$:

$$\alpha_m(\underline{s}_n(\tau), \underline{s}(\tau)) = \delta_{mn} , \qquad m = 1, ..., N ; \quad n = 1, ..., N + B .$$

The sum in (2.5) only goes from 1 to N because of the homogeneous Dirichlet boundary conditions on $\partial \Omega$.

In order to determine this approximation to $\underline{u}(\underline{x}, \tau)$ we need to find values for the unknowns $\underline{a}_1(\tau), \underline{s}_1(\tau), ..., \underline{a}_N(\tau), \underline{s}_N(\tau)$. The Moving Finite Element method does this by producing a weak or variational form of (2.3) for which the trial solution $\underline{u}^h$ takes the form of (2.5) and the test space is

9

the space in which the functions $\frac{\partial u_i^h}{\partial \tau}$ lie at each instant in time. In order to determine this space we differentiate (2.5) with respect to τ to give

$$\frac{\partial u_i^h}{\partial \tau} = \frac{\partial}{\partial \tau} \sum_{m=1}^{N} a_{mi}(\tau)\alpha_m(\underline{x}, \underline{s}(\tau))$$

$$= \sum_{m=1}^{N} \dot{a}_{mi}\alpha_m + \sum_{m=1}^{N} a_{mi}\frac{\partial \alpha_m}{\partial \underline{s}} \cdot \frac{d\underline{s}}{d\tau} \ ,$$

where this second term is present due to the time-dependence of each α_i through the time-dependence of the mesh $\underline{s}$, and the dot above a variable denotes differentiation with respect to τ. Hence

$$\frac{\partial u_i^h}{\partial \tau} = \sum_{m=1}^{N} \dot{a}_{mi}\alpha_m + \frac{\partial u_i^h}{\partial \underline{s}} \cdot \frac{d\underline{s}}{d\tau}$$

$$= \sum_{m=1}^{N} (\dot{a}_{mi}\alpha_m + \dot{\underline{s}}_m \cdot \frac{\partial u_i^h}{\partial \underline{s}_m}) \ , \tag{2.6}$$

and the following lemma allows this last term to be expressed in terms of more conventional derivatives.

Lemma 2.1

$$\frac{\partial u_i^h}{\partial \underline{s}_m} = -\alpha_m \underline{\nabla} u_i^h \ , \qquad and \ hence \qquad \frac{\partial u_i^h}{\partial s_{md}} = -\alpha_m \frac{\partial u_i^h}{\partial x_d} \qquad for \ d = 1, 2 \ . \tag{2.7}$$

Proof See [13] (or refer to lemma 3.1 for a proof of a similar result).

As is indicated above, the MFE method is derived by producing a weak form of (2.3), using the space in which the functions $\frac{\partial u_i^h}{\partial \tau}$ lie as the test space. An initial attempt to do this yields the following differential system:

$$< \sum_{m=1}^{N} (\dot{a}_{mi}\alpha_m + \dot{\underline{s}}_m \cdot \frac{\partial u_i^h}{\partial \underline{s}_m}), \alpha_n > = - < F_{,2i}(\underline{x}, \underline{u}^h, \underline{\nabla}\underline{u}^h), \alpha_n > + < \frac{d}{dx_j} F_{,3ij}(\underline{x}, \underline{u}^h, \underline{\nabla}\underline{u}^h), \alpha_n > \tag{2.8}$$

for $i = 1, 2$ and $n = 1, ..., N$, and

$$< \sum_{m=1}^{N} (\dot{a}_{mi}\alpha_m + \dot{\underline{s}}_m \cdot \frac{\partial u_i^h}{\partial \underline{s}_m}), \frac{\partial u_i^h}{\partial s_{ne}} > = - < F_{,2i}(\underline{x}, \underline{u}^h, \underline{\nabla}\underline{u}^h), \frac{\partial u_i^h}{\partial s_{ne}} > + < \frac{d}{dx_j} F_{,3ij}(\underline{x}, \underline{u}^h, \underline{\nabla}\underline{u}^h), \frac{\partial u_i^h}{\partial s_{ne}} >$$
$$\tag{2.9}$$

for $n = 1, ..., N$ and $e = 1, 2$. In this notation $< \cdot, \cdot >$ represents the usual L^2 inner product on Ω.

It should be noted at this point however that the second term on the right-hand-side of (2.9) is not generally defined, even in a distributional sense, when $u_i^h(\underline{x}, \tau)$ is piecewise linear. To overcome this difficulty we express equations (2.9) in a formally equivalent form which is defined when $u_i^h(\underline{x}, \tau)$ is piecewise linear for general choices of the function $F(\cdot, \cdot, \cdot)$. This is achieved by observing that

$$-\int_{\Omega} \{F_{,2i} - \frac{d}{dx_j}F_{,3ij}\}\frac{\partial u_i^h}{\partial s_{ne}} \ d\underline{x} = \int_{\Omega} \alpha_n \frac{\partial u_i^h}{\partial x_e}\{F_{,2i} - \frac{d}{dx_j}F_{,3ij}\} \ d\underline{x}$$

$$\text{(using lemma 2.1)}$$

$$= -\int_{\Omega} \{\alpha_n \frac{d}{dx_j}[\frac{\partial u_i^h}{\partial x_e}F_{,3ij} - F\delta_{ej}] + \alpha_n F_{,1e}\} \ d\underline{x} \tag{2.10}$$

10

(proof:

$$-\alpha_n \frac{d}{dx_j}[\frac{\partial u_i^h}{\partial x_e} F_{,3ij} - F\delta_{ej}] - \alpha_n F_{,1e} \;\; = \;\; -\alpha_n \frac{\partial u_i^h}{\partial x_e}\frac{d}{dx_j}[F_{,3ij}] - \alpha_n \frac{\partial^2 u_i^h}{\partial x_j \partial x_e} F_{,3ij} + \alpha_n F_{,1e}$$

$$+\alpha_n F_{,2i}\frac{\partial u_i^h}{\partial x_e} + \alpha_n F_{,3ik}\frac{\partial^2 u_i^h}{\partial x_e \partial x_k} - \alpha_n F_{,1e}$$

$$= \;\; -\alpha_n \frac{\partial u_i^h}{\partial x_e}\frac{d}{dx_j}[F_{,3ij}] + \alpha_n F_{,2i}\frac{\partial u_i^h}{\partial x_e} \;,$$

as required).

Using this new expression, (2.10), in (2.9), we may now derive from (2.8) and (2.9) the following definition of the Moving Finite Element equations for solving (2.3):

$$< \sum_{m=1}^{N}(\dot{a}_{mi}\alpha_m + \underline{\dot{s}}_m \cdot \frac{\partial u_i^h}{\partial \underline{s}_m}), \alpha_n > = - < F_{,2i}, \alpha_n > \; - \; < F_{,3ij}, \frac{\partial \alpha_n}{\partial x_j} > \tag{2.11}$$

for $i = 1, 2$ and $n = 1, ..., N$, and

$$< \sum_{m=1}^{N}(\dot{a}_{mi}\alpha_m + \underline{\dot{s}}_m \cdot \frac{\partial u_i^h}{\partial \underline{s}_m}), \frac{\partial u_i^h}{\partial s_{ne}} > = \int_\Omega [\frac{\partial u_i^h}{\partial x_e}F_{,3ij} - F\delta_{ej}]\frac{\partial \alpha_n}{\partial x_j} \, d\underline{x} - \int_\Omega F_{,1e}\alpha_n \, d\underline{x} \tag{2.12}$$

for $n = 1, ..., N$ and $e = 1, 2$. (Note that it is also possible to derive the above system of equations in an alternative fashion, using the original mollification technique of Miller which is described in [17]. This is entirely equivalent to the formal approach that is used here, which is a generalization of the integration by parts method first suggested by Mueller in [18].)

As has already been implied, the sets of equations (2.11) and (2.12) are referred to as the Moving Finite Element equations. They form a system of ordinary differential equations which may be written as

$$A(\underline{y})\underline{\dot{y}}(\tau) = \underline{g}(\underline{y}) \;, \tag{2.13}$$

where

$$\underline{y} = (a_{11}, a_{12}, s_{11}, s_{12}, ..., a_{N1}, a_{N2}, s_{N1}, s_{N2})^T,$$

$$\underline{\alpha}_1 = (\alpha_1, 0, \frac{\partial u_1^h}{\partial s_{11}}, \frac{\partial u_1^h}{\partial s_{12}}, ..., \alpha_N, 0, \frac{\partial u_1^h}{\partial s_{N1}}, \frac{\partial u_1^h}{\partial s_{N2}})^T,$$

$$\underline{\alpha}_2 = (0, \alpha_1, \frac{\partial u_2^h}{\partial s_{11}}, \frac{\partial u_2^h}{\partial s_{12}}, ..., 0, \alpha_N, \frac{\partial u_2^h}{\partial s_{N1}}, \frac{\partial u_2^h}{\partial s_{N2}})^T,$$

$$A = < \underline{\alpha}_1, \underline{\alpha}_1^T > + < \underline{\alpha}_2, \underline{\alpha}_2^T >$$

and $\underline{g}(\underline{y})$ is the known vector of right-hand-sides (from (2.11) and (2.12)). The matrix $A(\underline{y})$ is often called the "MFE mass matrix" by analogy with the usual Galerkin mass matrix.

Lemma 2.2 *The matrix $A(\underline{y})$ in (2.13) is positive semi-definite and is singular if and only if the MFE solution, $\underline{u}^h$, has a directional derivative which is continuous at one or more of the knot points $\underline{s}_1, ..., \underline{s}_N$.*

Proof Using (2.6), note that

$$\frac{\partial u_i^h}{\partial \tau} \;\; = \;\; \underline{\alpha}_i^T \underline{\dot{y}} \;\; = \;\; \underline{\dot{y}}^T \underline{\alpha}_i \;.$$

Hence for any choice of the vector $\underline{\dot{y}}$ we have

$$0 \leq \int_{\Omega} (\frac{\partial \underline{u}^h}{\partial \tau})^2 \, dV \;=\; \int_{\Omega} \underline{\dot{y}}^T \underline{\alpha}_i \underline{\alpha}_i^T \underline{\dot{y}} \, dV \;=\; \underline{\dot{y}}^T < \underline{\alpha}_i, \underline{\alpha}_i^T > \underline{\dot{y}} \;=\; \underline{\dot{y}}^T A \underline{\dot{y}} \qquad (2.14)$$

so A is indeed positive semi-definite (it can easily be shown to be symmetric).

Now observe from (2.14) that A is singular if and only if there is some vector $\underline{\dot{y}}(\neq 0)$ such that $\frac{\partial \underline{u}^h}{\partial \tau} = \underline{0}$. That is, $\underline{\dot{y}}^T \underline{\alpha}_i = 0$ for both $i = 1$ and $i = 2$. However $\underline{\dot{y}}^T \underline{\alpha}_i$ can be zero (for $\underline{\dot{y}} \neq 0$) if and only if some directional derivative of u_i is continuous at one or more of the nodes $\underline{s}_1(\tau), ..., \underline{s}_N(\tau)$ (by (2.6) and (2.7)). Hence A is singular if and only if there is at least one node for which the same directional derivative of both u_1 and u_2 is continuous. ///

When the matrix $A(\underline{y})$ in the system (2.13) is singular due to $\underline{u}^h$ having a continuous directional derivative at a knot point, the MFE solution will be described as "degenerate". Otherwise it will be said to be "non-degenerate", in which case $A(\underline{y})$ is strictly positive definite. The difficulties associated with degeneracy along with the possibility of the area of one or more of the elements in the mesh becoming non-positive as the knot points evolve are often cited as two of the major drawbacks of the MFE method. One approach to overcoming these difficulties is to attempt to influence the nodal motion by using penalty functions in the underlying minimization to which equations (2.11) and (2.12) correspond. This is the approach of Miller *et al* ([9], [16], [17]) and Mueller and Carey [19] for example. However, much of the work of Baines *et al* ([1], [2], [3], [14], [22]) suggests that the use of these awkward-to-handle penalty functions may not always be necessary. No such penalty functions will be used in this paper and so the only equations that we consider are those given by (2.13).

2.2 A Linear Example

Suppose that in (1.1), $F(\underline{x}, \underline{u}, \nabla \underline{u})$ is given by (1.2) and we retain the homogeneous displacement boundary conditions of subsection 2.1, then the parabolic differential equations (2.3) become

$$\frac{\partial u_i}{\partial \tau} = \rho b_i + \frac{\partial}{\partial x_j}[C_{ijk\ell} \frac{\partial u_k}{\partial x_\ell}] \quad (i = 1, 2) \,. \qquad (2.15)$$

(Here we have used the fact that

$$F_{,3ij} = C_{ijk\ell} \frac{\partial u_k}{\partial x_\ell}$$

due to the symmetry $C_{ijk\ell} = C_{k\ell ij}$.)

We may still look for a time-dependent piecewise linear solution to this problem of the form (2.5), and so the MFE equations (2.11) and (2.12) can again be derived. For this choice of F equations (2.11) reduce to

$$\sum_{m=1}^{N} \int_{\Omega} \alpha_m \alpha_n \, d\underline{x} \, \dot{a}_{mi} + \sum_{m=1}^{N} \sum_{d=1}^{2} \int_{\Omega} \frac{\partial u_i^h}{\partial s_{md}} \alpha_n \, d\underline{x} \, \dot{s}_{md} = \int_{\Omega} \rho b_i \alpha_n \, d\underline{x} - \int_{\Omega} C_{ijk\ell} \frac{\partial u_k^h}{\partial x_\ell} \frac{\partial \alpha_n}{\partial x_j} \, d\underline{x} \qquad (2.16)$$

for $i = 1, 2$ and $n = 1, ..., N$, and equations (2.12) reduce to

$$\sum_{m=1}^{N} \int_{\Omega} \alpha_m \frac{\partial u_i^h}{\partial s_{ne}} \, d\underline{x} \, \dot{a}_{mi} + \sum_{m=1}^{N} \sum_{d=1}^{2} \int_{\Omega} \frac{\partial u_i^h}{\partial s_{md}} \frac{\partial u_i^h}{\partial s_{ne}} \, d\underline{x} \, \dot{s}_{md} \;=\;$$

$$\int_{\Omega} \rho b_i \frac{\partial u_i^h}{\partial s_{ne}} \, d\underline{x} - \frac{1}{2} \int_{\Omega} \frac{\partial u_i^h}{\partial x_j} \frac{\partial u_k^h}{\partial x_\ell} \frac{\partial}{\partial x_e}[\alpha_n C_{ijk\ell}] \, d\underline{x} + \int_{\Omega} C_{ijk\ell} \frac{\partial u_k^h}{\partial x_\ell} \frac{\partial \alpha_n}{\partial x_j} \frac{\partial u_i^h}{\partial x_e} \, d\underline{x} \qquad (2.17)$$

for $n = 1, ..., N$ and $e = 1, 2$. (Again we have used the fact that

$$F_{,3ij} = C_{ijk\ell} \frac{\partial u_k}{\partial x_\ell} \ ,$$

and so the right-hand-side of (2.12) is equal to

$$\int_\Omega [\frac{\partial u_i^h}{\partial x_e} C_{ijk\ell} \frac{\partial u_k^h}{\partial x_\ell} \frac{\partial \alpha_n}{\partial x_j} - \frac{1}{2} \frac{\partial u_i^h}{\partial x_j} C_{ijk\ell} \frac{\partial u_k^h}{\partial x_\ell} \frac{\partial \alpha_n}{\partial x_e} + \rho b_i u_i \frac{\partial \alpha_n}{\partial x_e}] \, d\underline{x}$$
$$- \int_\Omega [\frac{1}{2} \frac{\partial u_i^h}{\partial x_j} \frac{\partial}{\partial x_e} C_{ijk\ell} \frac{\partial u_k^h}{\partial x_\ell} - \frac{\partial}{\partial x_e} (\rho b_i) u_i] \alpha_n \, d\underline{x}$$

for this choice of F.)

3 An Optimal Mesh Using the MFE Method

In this section we demonstrate that if the MFE method is applied to equations (2.3) in the manner described in subsection 2.1 then it is possible to obtain a steady solution of the MFE equations (2.13) which corresponds to an optimal solution of (1.1) on an *optimal mesh*. As with the previous section we will again assume that the boundary conditions associated with the problem are zero displacement conditions ($\underline{d} \equiv \underline{0}$ in (1.4)), and in the first subsection we derive the general result and in the second subsection we focus on the special case of the linear problem (2.15).

3.1 Optimality of the MFE Method

The main result of this subsection is to show that any stable, steady solution, $\underline{y}$ say, of (2.13) corresponds to a finite element function $\underline{u}^h$ which is a local minimizer of the stored energy functional in (1.1) over all choices of the mesh as well as over all finite element functions on that mesh.

In order to prove this result it will be helpful first to establish some more notation and then to prove a preliminary lemma.

- Suppose $n \in \{1, ..., N\}$ is the number of an internal node of a triangulation of the domain Ω. Then we will denote by $N(n)$ the number of elements in the triangulation that have this node as a vertex. Further, for $t = 1, ..., N(n)$, let $T(n, t)$ be a unique ordering of these $N(n)$ elements which have a vertex at $\underline{s}_n$, let $\Omega_{T(n,t)}$ be the region occupied by the triangle numbered $T(n, t)$ and let $A_{T(n,t)}$ be the area of this region.

- Given any triangle within a finite element mesh we may represent the vertices of that triangle by a local numbering as $\underline{\hat{s}}_0$, $\underline{\hat{s}}_1$ and $\underline{\hat{s}}_2$.

- We may also define a standard triangle, Δ, as the triangle whose vertices are $\underline{e}_0 = (0, 0)^T$, $\underline{e}_1 = (1, 0)^T$ and $\underline{e}_2 = (0, 1)^T$.

- Now define a mapping from an arbitrary element within a triangulation onto that standard triangle by

$$\underline{\xi}(\underline{x}, \underline{s}) = \sum_{\mu=0}^{2} \underline{e}_\mu \hat{\alpha}_\mu(\underline{x}, \underline{s}) \tag{3.1}$$

where $\hat{\alpha}_\mu(\underline{x}, \underline{s})$ is the usual linear basis function (but with a local numbering corresponding to a particular triangle) such that $\hat{\alpha}_\mu(\underline{s}_\nu, \underline{s}) = \delta_{\mu\nu}$, for $\mu, \nu \in \{0, 1, 2\}$.

- The inverse of this mapping is

$$\underline{x}(\underline{\xi},\underline{s}) = \sum_{\mu=0}^{2} \underline{\hat{s}}_{\mu} \tilde{\alpha}_{\mu}(\underline{\xi}) \tag{3.2}$$

where the $\tilde{\alpha}_{\mu}(\underline{\xi})$ are the piecewise linear basis functions on the standard triangle such that $\tilde{\alpha}_{\mu}(\underline{e}_{\nu}) = \delta_{\mu\nu}$. (Note that $\tilde{\alpha}_{\mu}(\underline{\xi}) \equiv \hat{\alpha}_{\mu}(\underline{x}(\underline{\xi},\underline{s}),\underline{s})$.)

Lemma 3.1 *Given a triangle with vertices $\underline{\hat{s}}_0$, $\underline{\hat{s}}_1$, $\underline{\hat{s}}_2$ and area $A(\underline{\hat{s}}_0,\underline{\hat{s}}_1,\underline{\hat{s}}_2)$, then*

$$\frac{\partial A}{\partial \hat{s}_{\nu e}} = \frac{\partial \hat{\alpha}_{\nu}}{\partial x_e} A \qquad \text{for } \nu \in \{0,1,2\} \text{ and } e \in \{1,2\}.$$

Proof Without loss of generality consider the case $\nu = 0$. Because each of $\hat{\alpha}_0$, $\hat{\alpha}_1$ and $\hat{\alpha}_2$ are area coordinates we know that

$$\hat{\alpha}_0(\underline{x}) = A(\underline{x},\underline{\hat{s}}_1,\underline{\hat{s}}_2)/A(\underline{\hat{s}}_0,\underline{\hat{s}}_1,\underline{\hat{s}}_2) . \tag{3.3}$$

Moreover, since $\hat{\alpha}_0$ is affine we know that $\frac{\partial \hat{\alpha}_0}{\partial x_e}$ is independent of $\underline{x}$ and so from (3.3) $\frac{\partial}{\partial x_e}A(\underline{x},\underline{\hat{s}}_1,\underline{\hat{s}}_2)$ must be independent of $\underline{x}$. This implies that $\frac{\partial}{\partial \hat{s}_{0e}}A(\underline{\hat{s}}_0,\underline{\hat{s}}_1,\underline{\hat{s}}_2)$ must be independent of $\underline{\hat{s}}_0$ and therefore that

$$\frac{\partial}{\partial x_e}A(\underline{x},\underline{\hat{s}}_1,\underline{\hat{s}}_2) = \frac{\partial}{\partial \hat{s}_{0e}}A(\underline{\hat{s}}_0,\underline{\hat{s}}_1,\underline{\hat{s}}_2) .$$

Hence

$$\frac{\partial \hat{\alpha}_0}{\partial x_e} = \frac{\partial A}{\partial \hat{s}_{0e}}/A .$$

Since this argument is valid for any choice of $\nu \in \{0,1,2\}$, the result is proved. ///

We are now in a position to prove the following theorem.

Theorem 3.2 *Suppose the stored energy functional $E(\underline{u}) = \int_{\Omega} F(\underline{x},\underline{u},\nabla \underline{u}) \, d\underline{x}$ has a minimizer $\underline{u}(\underline{x})$ which satisfies the corresponding Euler-Lagrange equations (2.1). Let*

$$\underline{u}^h(\underline{x},\tau) = \sum_{m=1}^{N} \underline{a}_m(\tau)\alpha_m(\underline{x},\underline{s}(\tau))$$

be a continuous piecewise linear approximation to this minimizer on a mesh $\underline{s}(\tau)$ with N free internal knots $\underline{s}_1(\tau), ..., \underline{s}_N(\tau)$. Also let

$$\underline{y} = (a_{11}, a_{12}, s_{11}, s_{12}, ..., a_{N1}, a_{N2}, s_{N1}, s_{N2})^T$$

and $I(\underline{y}) = E(\underline{u}^h)$. Then

$$\nabla I(\underline{y}) = -\underline{g}(\underline{y}) , \tag{3.4}$$

for $\underline{g}(\underline{y})$ as in (2.13).

Proof We begin by observing, from (2.11) and (2.12), that $\underline{g}(\underline{y})$ consists of the following components:

$$-\int_{\Omega} F_{,2i}\alpha_n \, d\underline{x} - \int_{\Omega} F_{,3ij}\frac{\partial \alpha_n}{\partial x_j} \, d\underline{x} \tag{3.5}$$

for $i = 1,2$ and $n = 1, ..., N$, and

$$\int_{\Omega}[\frac{\partial u_i^h}{\partial x_e}F_{,3ij} - F\delta_{ej}]\frac{\partial \alpha_n}{\partial x_j} \, d\underline{x} - \int_{\Omega} F_{,1e}\alpha_n \, d\underline{x} \tag{3.6}$$

14

for $n = 1, ..., N$ and $e = 1, 2$. We now show that the components of $\underline{\nabla} I(\underline{y})$ are as claimed in (3.4) by demonstrating that (3.5) is $-\frac{\partial I}{\partial a_{ni}}$ for $i = 1, 2$ and $n = 1, ..., N$, and (3.6) is $-\frac{\partial I}{\partial s_{ne}}$ for $n = 1, ..., N$ and $e = 1, 2$.

For the first of these two cases it immediately follows from the definition of $I(\underline{y})$ that for $i = 1, 2$ and $n = 1, ..., N$,

$$\frac{\partial I}{\partial a_{ni}} = \int_\Omega [F_{,2i}(\underline{x}, \underline{u}^h, \underline{\nabla} \underline{u}^h)\alpha_n + F_{,3ij}(\underline{x}, \underline{u}^h, \underline{\nabla} \underline{u}^h)\frac{\partial \alpha_n}{\partial x_j}] \, d\underline{x} \, ,$$

which is equal to -1 times (3.5) as required.

For the other case, for $n = 1, ..., N$ and $e = 1, 2$, we have

$$
\begin{aligned}
\frac{\partial I}{\partial s_{ne}} &= \frac{\partial}{\partial s_{ne}} \sum_{t=1}^{N(n)} \int_{\Omega_{T(n,t)}} F(\underline{x}, \underline{u}^h, \underline{\nabla} \underline{u}^h) \, d\underline{x} \\
&= \sum_{t=1}^{N(n)} \frac{\partial}{\partial s_{ne}} \int_\Delta F(\underline{x}(\underline{\xi}, \underline{s}), \underline{u}^h(\underline{x}(\underline{\xi}, \underline{s}), \underline{s}), \underline{D}(\underline{a}, \underline{s}))|\frac{d\underline{x}}{d\underline{\xi}}| \, d\underline{\xi} \\
&= \sum_{t=1}^{N(n)} \{ \int_\Delta F\frac{\partial}{\partial s_{ne}}|\frac{d\underline{x}}{d\underline{\xi}}| \, d\underline{\xi} + \int_\Delta F_{,1i}\frac{\partial x_i}{\partial s_{ne}}|\frac{d\underline{x}}{d\underline{\xi}}| \, d\underline{\xi} + \int_\Delta F_{,2i}[\frac{\partial u_i^h}{\partial x_j}\frac{\partial x_j}{\partial s_{ne}} + \frac{\partial u_i^h}{\partial s_{ne}}]|\frac{d\underline{x}}{d\underline{\xi}}| \, d\underline{\xi} + \\
&\qquad\qquad \int_\Delta F_{,3ij}\frac{\partial D_{ij}}{\partial s_{ne}}|\frac{d\underline{x}}{d\underline{\xi}}| \, d\underline{\xi} \} \, ,
\end{aligned}
$$

where $\underline{x}(\underline{\xi}, \underline{s})$ is given by (3.2), Δ is a standard triangle, and D_{pq} represents the value of $\frac{\partial u_p^h}{\partial x_q}$ restricted to the triangle $T(n, t)$. (Note that this value is independent of $\underline{x}$ since we are using piecewise linear finite elements.)

We may now make use of the fact that the Jacobian, $|\frac{d\underline{x}}{d\underline{\xi}}|$, in the above transformation is equal to $2A_{T(n,t)}$ on each triangle and so, using lemma 3.1,

$$\frac{\partial}{\partial s_{ne}}|\frac{d\underline{x}}{d\underline{\xi}}| = \frac{\partial \alpha_n}{\partial x_e}|\frac{d\underline{x}}{d\underline{\xi}}| \, .$$

In addition we may use lemma 2.1 and the fact that $\underline{u}^h(\underline{x})$ is piecewise linear to deduce that, on each triangle $T(n, t)$,

$$\frac{\partial D_{ij}}{\partial s_{ne}} = \frac{\partial}{\partial s_{ne}}[\frac{\partial u_i^h}{\partial x_j}] = \frac{\partial}{\partial x_j}[\frac{\partial u_i^h}{\partial s_{ne}}] = \frac{\partial}{\partial x_j}[-\alpha_n\frac{\partial u_i^h}{\partial x_e}] = -\frac{\partial \alpha_n}{\partial x_j}\frac{\partial u_i^h}{\partial x_e} \, .$$

We can now deduce that

$$
\begin{aligned}
\frac{\partial I}{\partial s_{ne}} &= \sum_{t=1}^{N(n)} \int_\Delta \{F\frac{\partial \alpha_n}{\partial x_e} + F_{,1i}\delta_{ie}\alpha_n + F_{,2i}[\frac{\partial u_i^h}{\partial x_j}\delta_{je}\alpha_n + \frac{\partial u_i^h}{\partial s_{ne}}] - F_{,3ij}\frac{\partial \alpha_n}{\partial x_j}\frac{\partial u_i^h}{\partial x_e}\}|\frac{d\underline{x}}{d\underline{\xi}}| \, d\underline{\xi} \\
&\qquad \text{(using the fact that, by (3.2), } \frac{\partial x_k}{\partial s_{ne}} = \delta_{ke}\alpha_n) \\
&= \sum_{t=1}^{N(n)} \int_{\Omega_{T(n,t)}} \{F\frac{\partial \alpha_n}{\partial x_e} + F_{,1e}\alpha_n - F_{,3ij}\frac{\partial \alpha_n}{\partial x_j}\frac{\partial u_i^h}{\partial x_e}\} \, d\underline{x} \\
&\qquad \text{(again using lemma 2.1)} \\
&= \int_\Omega [F\delta_{ej} - \frac{\partial u_i^h}{\partial x_e}F_{,3ij}]\frac{\partial \alpha_n}{\partial x_j} \, d\underline{x} + \int_\Omega F_{,1e}\alpha_n \, d\underline{x} \, ,
\end{aligned}
$$

15

which is equal to -1 times (3.6) as required. ///

The above theorem tells us that when we have obtained a non-degenerate steady solution of the Moving Finite Element Equations (2.13), and so $\underline{g}(\underline{y}) = \underline{0}$, then we must be at a stationary value of the functional $I(\underline{y})$, which is equal to $E(\underline{u}^h)$. In order to show that this stationary point is in fact a local energy minimizer we must also show that the Hessian of I is positive definite at this point. This means that the Jacobian of $\underline{g}(\underline{y})$, which by (3.4) must be symmetric, must be shown to be negative definite at such a steady solution of the Moving Finite Element equations. This is done in the following proof.

Corollary 3.3 *Any non-degenerate, asymptotically stable, steady solution of the Moving Finite Element equations (2.13) for solving the problem (2.3) is an optimal finite element solution of the elastostatic problem (1.1) on an optimal mesh.*

Proof Suppose $\underline{y}_0$ is such a non-degenerate, asymptotically stable, steady solution of (2.13), then $A(\underline{y}_0)$ is positive definite (by lemma 2.2). Now take a small perturbation of $\underline{y}_0$, given by $\underline{y}_0 + \epsilon \underline{y}_1$, so that (2.13) becomes

$$A(\underline{y}_0 + \epsilon \underline{y}_1)(\underline{\dot{y}}_0 + \epsilon \underline{\dot{y}}_1) = \underline{g}(\underline{y}_0 + \epsilon \underline{y}_1) \,.$$

Linearizing this about $\underline{y}_0$ gives

$$\underline{\dot{y}}_1 = A^{-1}(\underline{y}_0) \, D\underline{g}(\underline{y}_0) \, \underline{y}_1 \,,$$

where $D\underline{g}(\underline{y}_0)$ is the Jacobian of $\underline{g}$ with respect to $\underline{y}$ evaluated at $\underline{y}_0$. Now, the asymptotic stability of $\underline{y}_0$ implies that all eigenvalues of the product $A^{-1}(\underline{y}_0)D\underline{g}(\underline{y}_0)$ must have negative real parts. Since $A^{-1}(\underline{y}_0)$ is strictly positive definite we deduce that $D\underline{g}(\underline{y}_0)$ must be negative definite and so, from (3.4), the Hessian of $I(\underline{y})$ must be positive definite at $\underline{y}_0$, as required. ///

The outcome of this therefore means that if we apply the approach outlined in subsection 2.1 to solving the problem (2.3), then any steady solution of (2.13) that we obtain will be locally optimal on an optimal mesh in the sense that it will be a local minimizer of the functional in (1.1) over all variations in both the nodal displacement values and the nodal positions.

3.2   The Linear Example

We now return to the specific example where $F(\underline{x}, \underline{u}, \nabla \underline{u})$ in (1.1) is given by (1.2), so the parabolic equations (2.3) reduce to the linear form (2.15). In this case the results of the previous section show that any stable steady solutions of the MFE equations (2.16) and (2.17) will be local minimizers of

$$\frac{1}{2} \int_\Omega \frac{\partial u_i^h}{\partial x_j} C_{ijk\ell} \frac{\partial u_k^h}{\partial x_\ell} \, d\underline{x} - \int_\Omega \rho b_i u_i^h \, d\underline{x} \tag{3.7}$$

over local variations in each $\underline{a}_k$ and $\underline{s}_k$ for $k = 1, ..., N$.

For this particular example of a linear elasticity problem it is possible to derive a further corollary to theorem 3.2.

Corollary 3.4 *Let $\underline{u}(\underline{x})$ be the unique steady solution of (2.15) subject to zero displacement boundary conditions on $\partial \Omega$. (See [6, section 2.2], for example, for a proof of this existence and uniqueness result.) Then if $\underline{\tilde{u}}^h(\underline{x})$ is a stable steady solution of the MFE equations (2.16) and (2.17), it must be a local minimizer of the error, $\underline{u}(\underline{x}) - \underline{u}^h(\underline{x})$, in the energy norm:*

$$\| \, \underline{e} \, \|_E^2 = \frac{1}{2} \int_\Omega \frac{\partial e_i}{\partial x_j} C_{ijk\ell} \frac{\partial e_k}{\partial x_\ell} \, d\underline{x} \,. \tag{3.8}$$

16

Proof First observe that

$$
\begin{aligned}
\| \underline{u} - \underline{u}^h \|_E^2 &= \frac{1}{2} \int_\Omega \frac{\partial}{\partial x_j}(u_i - u_i^h) C_{ijk\ell} \frac{\partial}{\partial x_\ell}(u_k - u_k^h) \, d\underline{x} \\
&= \frac{1}{2} \int_\Omega \frac{\partial u_i^h}{\partial x_j} C_{ijk\ell} \frac{\partial u_k^h}{\partial x_\ell} \, d\underline{x} - \frac{1}{2} \int_\Omega [\frac{\partial u_i}{\partial x_j} C_{ijk\ell} \frac{\partial u_k^h}{\partial x_\ell} + \frac{\partial u_i^h}{\partial x_j} C_{ijk\ell} \frac{\partial u_k}{\partial x_\ell}] \, d\underline{x} + \\
&\quad \frac{1}{2} \int_\Omega \frac{\partial u_i}{\partial x_j} C_{ijk\ell} \frac{\partial u_k}{\partial x_\ell} \, d\underline{x} \\
&= E(\underline{u}^h) + \int_\Omega \rho b_i u_i^h \, d\underline{x} - \int_\Omega \frac{\partial u_i^h}{\partial x_j} C_{ijk\ell} \frac{\partial u_k}{\partial x_\ell} \, d\underline{x} + \frac{1}{2} \int_\Omega \frac{\partial u_i}{\partial x_j} C_{ijk\ell} \frac{\partial u_k}{\partial x_\ell} \, d\underline{x} \\
&\quad \text{(using the symmetry } C_{ijk\ell} = C_{k\ell ij}) \\
&= E(\underline{u}^h) + \int_\Omega \{ u_i^h \frac{\partial}{\partial x_j}[C_{ijk\ell} \frac{\partial u_k}{\partial x_\ell}] + \rho b_i u_i^h \} \, d\underline{x} + \frac{1}{2} \int_\Omega \frac{\partial u_i}{\partial x_j} C_{ijk\ell} \frac{\partial u_k}{\partial x_\ell} \, d\underline{x} \\
&= E(\underline{u}^h) + \frac{1}{2} \int_\Omega \frac{\partial u_i}{\partial x_j} C_{ijk\ell} \frac{\partial u_k}{\partial x_\ell} \, d\underline{x}
\end{aligned}
$$

(since $\underline{u}$ is a steady solution of (2.15)). Hence any choice of $\{\underline{a}_k, \underline{s}_k : \ k = 1, ..., N\}$ which minimizes $E(\underline{u}^h)$ must also minimize $\| \underline{u} - \underline{u}^h \|_E^2$. But from the result of corollary 3.3 it is known that $\tilde{\underline{u}}^h(\underline{x})$ corresponds to just such a choice, and so $\tilde{\underline{u}}^h(\underline{x})$ must also be a minimizer of this error in the energy norm (3.8), as claimed. $///$

This result shows that for linear elastic structural analysis problems, the optimality results of theorem 3.2 and corollary 3.3 imply that the Moving Finite Element method can yield a best approximation to $\underline{u}(\underline{x})$ in the sense that the error is minimized in the energy norm (3.8). This local minimum is again over all variations in the mesh as well as in the representation of the solution on that mesh.

4 Examples and Discussion

We conclude the paper by introducing two numerical examples to verify the results of the preceding sections and then by making a number of comments on the possible practical applications and limitations of these results. In the following subsection the first example falls into the category of those problems considered above: with zero displacement boundary conditions everywhere. The second problem is perhaps a little more practical and makes use of traction boundary conditions: although these are not considered explicitly in the above theory we see that few complications arise as a result of their inclusion. In both cases it is demonstrated that the Moving Finite Element method can indeed yield stable steady solutions which we may therefore deduce (and verify) are locally optimal solutions on locally optimal meshes.

4.1 Computational Examples

The examples in this subsection are chosen for their simplicity and aim to illustrate the theoretical results derived above. For this reason only the linear problem (2.15), whose exact steady solution is the unique minimizer of (3.7), is considered computationally.

For the first example the domain, Ω, is $(0, 1) \times (0, 1)$ and the elasticity tensor, **C**, is chosen to correspond to an isotropic material with a non-dimensionalized Young's modulus $E = 100$ and Poisson ratio $\nu = 0.001$. The values of $\rho b_1(\underline{x})$ and $\rho b_2(\underline{x})$ in (2.15) and (3.7) are chosen so as to yield the exact solution

$$ u_1(\underline{x}) = u_2(\underline{x}) = 64 x_1^2(1 - x_1) x_2^2(1 - x_2) $$

which satisfies the zero displacement boundary condition ($\underline{d} \equiv \underline{0}$ in (1.4)) everywhere on $\partial\Omega$. When the resulting MFE equations (2.13) are solved using regular initial data on the regular initial mesh shown in figure 1, the solution $\underline{y}(\tau)$ does indeed tend to a steady-state as $\tau \to \infty$. The second mesh in figure 1 depicts the steady nodal positions and table 1 shows the final values of all of the degrees of freedom (node positions, $\underline{s}_i$, and displacements, $\underline{a}_i$, for $i = 1,...,25$).

Having obtained a stable, steady MFE solution it is now possible to verify that it is optimal. This may be done with the aid of some appropriate minimization software, such as the NAG library minimization routine E04JAF ([20]) for example. Using this subroutine one can show that the MFE solution given in table 1 is indeed a local minimizer of both the total stored energy (3.7), and the error in the energy norm (3.8). (Note that this example was chosen so as to have a known analytic solution, $\underline{u}(\underline{x})$, and so it is possible to verify explicitly that the error $\| \underline{u}(\underline{x}) - \underline{u}^h(\underline{x}) \|_E$ is minimized.) In fact it turns out that the error in the Moving Finite Element solution is about 20% smaller than the error obtained by a conventional finite element analysis on the original grid (the first grid in figure 1).

We now consider a slightly more realistic problem which involves the use of traction boundary conditions. Figure 2 depicts an overhanging cantilever beam with a vertical concentrated load at the end of the cantilever. An initial finite element mesh is also shown. When this problem is solved using the same elasticity tensor as in the previous example we again obtain a steady MFE solution as $\tau \to \infty$. The final values of the 122 degrees of freedom ($\underline{s}_i$ and $\underline{a}_i$ for $i = 1,...,21$, and $\underline{a}_i$ for $i = 22,...,40$) are tabulated in table 2 and the corresponding final mesh is illustrated in figure 3. Note that the definition of the Moving Finite Element equations (2.13) has had to be altered slightly to take into account the fact that some of the boundary, $\partial_\theta \subset \partial\Omega$ say, has traction conditions of the form

$$n_j C_{ijk\ell} \frac{\partial u_k}{\partial x_\ell} = n_j \sigma_{ij} = \theta_i \; , \tag{4.9}$$

applied on it (where $\underline{n}$ is the outward unit normal vector). This means that those nodes (numbered 22 to 40 in this case) on this part of the boundary no longer have their displacement values prescribed and so these become additional dependent variables in (2.13). For simplicity we have chosen still to keep the positions of all of the nodes on the boundary fixed although in theory these too could be allowed to vary (along the boundary). For a more detailed description of how the derivation of the MFE equations is effected by the use of these boundary conditions see [11] or [12].

Again we may consider the stable steady MFE solution that has been tabulated, this time in table 2, and verify that it too is optimal. Since for this example we do not know the exact solution of the problem we are only able to verify that our discrete solution minimizes the stored energy function, which for this problem is

$$\frac{1}{2} \int_\Omega \frac{\partial u_i}{\partial x_j} C_{ijk\ell} \frac{\partial u_k}{\partial x_\ell} \, d\underline{x} - \int_\Omega \rho b_i u_i \, d\underline{x} - \int_{\partial_\theta} \theta_i u_i \, ds \; . \tag{4.10}$$

Here ∂_θ and θ_i are as in (4.9) and the addition of the extra boundary integral term to (3.7) is due to these traction boundary conditions (4.9). Use of the NAG routine E04JAF does indeed verify that the solution given in table 2 is a local minimizer of (4.10) over all variations in nodal positions, $\underline{s}_i$ ($i = 1,...,21$), and displacements, $\underline{a}_i$ ($i = 1,...,40$).

4.2 Discussion

On first inspection it may appear that the optimal mesh shown in figure 3 is not particularly ideal for representing the solution to this overhanging cantilever beam problem. It is an optimal mesh however. The reason for this apparent inconsistency is that the mesh derived in solving this problem is constrained to be of the same geometric topology as the initial regular mesh shown in figure

2. This is undoubtedly one of the practical drawbacks of the MFE method as outlined here. A possible approach to overcoming this is to allow occasional remeshing of the node points so as to alter the connectivity, $\mathcal{C}$, of the grid (see [15] for example, where the additional feature of adding and removing nodes is also considered). Another drawback in this particular example is that the movement of the nodes is restricted only to those points lying inside the domain Ω. This causes a significant amount of stretching to occur in a number of elements situated next to the boundary of the domain; something which would be alleviated if nodes on the boundary were free to move along it. In theory there is no reason why constrained motion of nodes along the boundary cannot be allowed in the MFE method (see [11] and [12] for example) and the theoretical results of section 3 can be extended accordingly. The practical difficulties of implementing this in software are more non-trivial however (although the importance of allowing such tangential motion of the boundary nodes suggests that this programming effort is likely to be worthwhile).

Another practical drawback of using the Moving Finite Element method as described in section 2 is the computational overhead associated with it. By allowing the nodal positions to become degrees of freedom we effectively double the size of the discrete problem that must be solved. Moreover, since equations (2.13) are dependent upon the artificial time parameter τ, the work involved in solving them is significantly more than that associated with a more conventional discretization of (1.1) or (2.1). This does not mean however that the method and the results of section 3 cannot be of significant practical value.

Firstly, there is no need to solve equations (2.13) with particularly high accuracy: a nearly steady solution (within a couple of percent of the true steady solution for example) will provide an almost optimal mesh, and a good initial estimate of the displacements, which can be used with a standard finite element analysis code. This will allow a considerably more accurate solution to be obtained than would be possible on a uniform mesh.

Secondly, and perhaps more practically, equations (2.13) need only be solved using a coarse finite element mesh. This would yield an optimal coarse initial mesh upon which to base an adaptive finite element analysis using h-refinement. Since the efficiency of most h-refinement algorithms is heavily dependent upon the choice of coarse mesh that is used and it is known that this coarse mesh is optimal, it is to be expected that this combination of r- and h-refinement should work well. Figure 4 illustrates how this looks in practice by showing the effect of local h-refinement on the grid that was produced in the solution to the cantilever beam example (figure 3) above. Those elements with the largest contributions to the functional in (1.1) have been found at very little extra computational cost and then locally refined, to give the mesh shown. A more accurate solution can now be found on this mesh in the usual way.

The numerical examples discussed above and in the previous subsection are both for isotropic linear elastic problems however the theory of sections 2 and 3 extends to non-isotropic, nonlinear cases too. Whilst these results are therefore of some significance in their own right it remains to be seen whether or not the Moving Finite Element method has a practical role to play in structural analysis. This will depend very much upon whether it is possible to utilize its strong theoretical properties to produce reliable and efficient numerical software, possibly in conjunction with other forms of adaptive refinement as suggested in figure 4. Further work is clearly needed in this area.

A final point which has not been addressed at all in this paper is that of what should be done if the solution of equations (2.13) is such that one or more of the finite elements shrinks to zero area as τ evolves. In theory there is nothing to prevent such an occurrence although it rarely appears to happen in practice. It would be useful understand exactly how and when this will occur and to implement a suitable strategy, such as regridding the mesh points, for when it does.

References

[1] M J Baines (1985). *Locally Adaptive Moving Finite Elements.* Numerical Methods for Fluid Dynamics II (eds. K W Morton & M J Baines), Oxford University Press.

[2] M J Baines and A J Wathen (1986). *Moving Finite Element Modelling of Compressible Flow.* Applied Num. Maths., 2, 495–514.

[3] M J Baines and A J Wathen (1988). *Moving Finite Element Methods for Evolutionary Problems. I. Theory.* J. of Comp. Phys., 79, 245–269.

[4] I Babuška, B Szabó and I N Katz (1981). *The p-version of the Finite Element Method.* SIAM J. Num. Anal., 18, 515–545.

[5] Jung-Ho Cheng (1993). *Adaptive Grid Optimization for Structural Analysis – Geometry-Based Approach.* Comput. Meth. Appl. Mech. Eng., 107, 1–22.

[6] P G Ciarlet (1983). *Lectures on Three Dimensional Elasticity.* Springer-Verlag.

[7] C A Fellipa (1976). *Optimization of Finite Element Grids by Direct Energy Search.* App. Math. Modelling, 1, 93–96.

[8] C A Fellipa (1977). *Numerical Experiments in Finite Element Grid Optimization by Direct Energy Search.* App. Math. Modelling, 1, 239–244.

[9] R J Gelinas, S K Doss and K Miller (1981). *The Moving Finite Element Method: Application to General Partial Differential Equations with Multiple Large Gradients.* J. of Comp. Phys., 40, 202–249.

[10] P K Jimack (1992). *On Steady and Large Time Solutions of the Semi-Discrete Moving Finite Element Equations for One-Dimensional Diffusion Equations.* IMA J. Num. Anal., 12, 545–564.

[11] P K Jimack (1993). *A Best Approximation Property of the Moving Finite Element Method.* School of Computer Studies Report 93.35, University of Leeds. (Submitted to SIAM J. Num. Anal.)

[12] P K Jimack (1994). *An Optimal Finite Element Mesh for Linear Elastic Structural Analysis.* In "Advances in Post and Preprocessing for Finite Element Technology" (eds. M. Papadrakakis & B.H.V. Topping), Civil-Comp Press.

[13] P K Jimack and A J Wathen(1991). *Temporal Derivatives in the Finite Element Method on Continuously Deforming Grids.* SIAM J. Num. Anal., 28, 990–1003.

[14] I W Johnson, A J Wathen and M J Baines (1988). *Moving Finite Element Methods for Evolutionary Problems. II. Applications.* J. of Comp. Phys., 79, 270–297.

[15] A Kuprat (1992). *Creation and Annihilation of Nodes for the Moving Finite Element Method.* Ph.D. Thesis, University of California at Berkeley. Unpublished.

[16] K Miller and R Miller (1981). *Moving Finite Elements, Part I.* SIAM J. Num. Anal., 18, 1019–1032.

[17] K Miller (1981). *Moving Finite Elements, Part II.* SIAM J. Num. Anal., 18, 1033–1057.

[18] A C Mueller (1983). *Continuously Deforming Finite Element Methods for Transport Problems.* Ph.D. Thesis, University of Austin, Texas. Unpublished.

[19] A C Mueller and G F Carey (1985). *Continuously Deforming Finite Elements.* Int. J. Num. Meth. Eng., 21, 2099–2126.

[20] Numerical Algorithms Group Limited (1993) *The NAG Fortran Library Manual – Mark 14.*

[21] J W Tang and D J Turke (1977). *Characteristics of Optimal Grids.* Comput. Meth. Appl. Mech. Eng., 11, 31–37.

[22] A J Wathen and M J Baines (1985). *On the Structure of the Moving Finite Element Equations.* IMA J. Num. Anal., 5, 161–182.

[23] J Z Zhu and O C Zienkiewicz (1988). *Adaptive Techniques in the Finite Element Method.* Comm. Appl. Num. Methods, 4, 197–204.
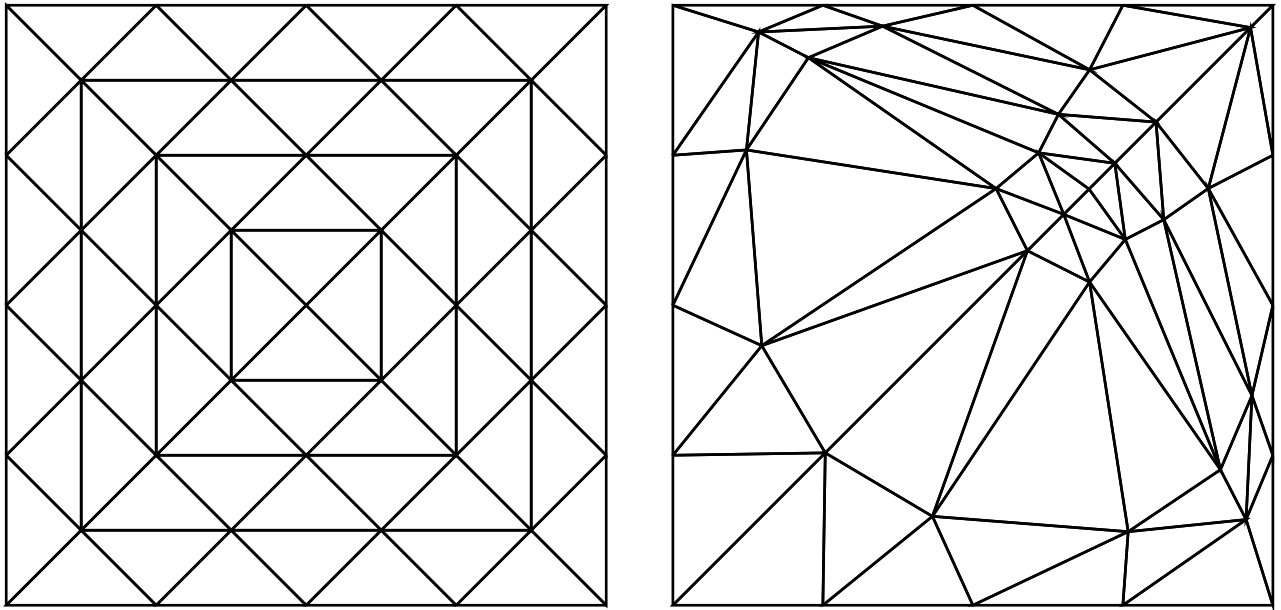
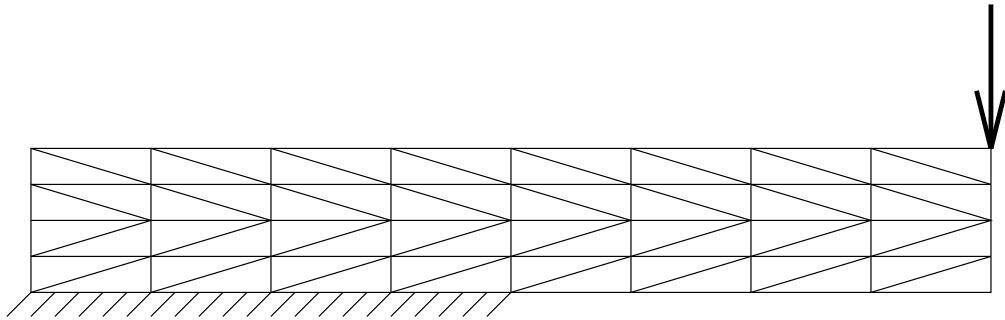Figure 1: The initial and final meshes in the first example.

Figure 2: The initial mesh for an overhanging cantilever beam with a vertical concentrated load at the end of the cantilever (the second example).
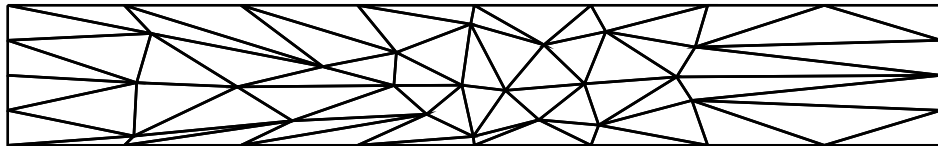

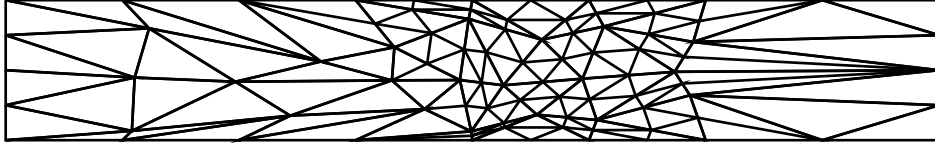Figure 3: The final mesh in the second example.

Figure 4: The effect of local h-refinement on the final mesh in the second example.

i	$\underline{s}_i$	$\underline{a}_i$
1	$(0.69364970, 0.69364970)^T$	$(1.3550871, 1.3550871)^T$
2	$(0.22589896, 0.91261447)^T$	$(0.18986173, 0.19742885)^T$
3	$(0.59090799, 0.59090799)^T$	$(1.2750743, 1.2750743)^T$
4	$(0.91261447, 0.22589896)^T$	$(0.19742885, 0.18986173)^T$
5	$(0.80526143, 0.80526143)^T$	$(1.0431178, 1.0431178)^T$
6	$(0.53865798, 0.69448498)^T$	$(1.2403749, 1.2463933)^T$
7	$(0.60966146, 0.75403842)^T$	$(1.2843933, 1.2818275)^T$
8	$(0.65144442, 0.65144442)^T$	$(1.3733659, 1.3733659)^T$
9	$(0.14283922, 0.95538455)^T$	$(0.044817489, 0.044377864)^T$
10	$(0.12260433, 0.75885079)^T$	$(0.11494611, 0.11378281)^T$
11	$(0.14819209, 0.43261430)^T$	$(0.14421655, 0.14233981)^T$
12	$(0.25397459, 0.25397459)^T$	$(0.13040246, 0.13040246)^T$
13	$(0.69448498, 0.53865798)^T$	$(1.2463933, 1.2403749)^T$
14	$(0.75403842, 0.60966146)^T$	$(1.2818275, 1.2843933)^T$
15	$(0.43261430, 0.14819209)^T$	$(0.14233981, 0.14421655)^T$
16	$(0.75885079, 0.12260433)^T$	$(0.11378281, 0.11494611)^T$
17	$(0.95538455, 0.14283922)^T$	$(0.044377864, 0.044817489)^T$
18	$(0.81816556, 0.64261816)^T$	$(1.1445529, 1.1530219)^T$
19	$(0.73657273, 0.73657273)^T$	$(1.2926651, 1.2926651)^T$
20	$(0.64261816, 0.81816556)^T$	$(1.1530219, 1.1445529)^T$
21	$(0.96515183, 0.34947743)^T$	$(0.17348793, 0.16987146)^T$
22	$(0.89237610, 0.69457314)^T$	$(0.80121411, 0.81922981)^T$
23	$(0.96278242, 0.96278242)^T$	$(0.15449516, 0.15449516)^T$
24	$(0.69457314, 0.89237610)^T$	$(0.81922981, 0.80121411)^T$
25	$(0.34947743, 0.96515183)^T$	$(0.16987146, 0.17348793)^T$

Table 1: The values of the 100 degrees of freedom at the steady MFE solution to the first example problem.

i	$\underline{s}_i$	$\underline{a}_i$
1	$(0.61456606, 0.47923320)^T$	$(0.0057128317, 0.0024057717)^T$
2	$(1.3508914, 0.33709922)^T$	$(0.018124359, 0.0039853696)^T$
3	$(1.6658348, 0.39799753)^T$	$(0.034182316, 0.0039527141)^T$
4	$(1.9843904, 0.51931928)^T$	$(0.083173394, -0.020636952)^T$
5	$(2.2980489, 0.43062728)^T$	$(0.093319382, -0.11889211)^T$
6	$(2.5632998, 0.48729489)^T$	$(0.13994718, -0.24150486)^T$
7	$(2.9466186, 0.42107679)^T$	$(0.12854469, -0.49384140)^T$
8	$(0.55265310, 0.26833740)^T$	$(0.0040340932, 0.0014452070)^T$
9	$(0.98419625, 0.25049591)^T$	$(0.0083095121, 0.0028406895)^T$
10	$(1.6552233, 0.25631920)^T$	$(0.019191152, 0.0025423956)^T$
11	$(1.9466160, 0.25760568)^T$	$(0.027981717, -0.013151568)^T$
12	$(2.1329383, 0.23533503)^T$	$(0.025296867, -0.054448789)^T$
13	$(2.4721697, 0.26354485)^T$	$(0.026298447, -0.19275032)^T$
14	$(2.8670582, 0.29304043)^T$	$(0.037755895, -0.43405716)^T$
15	$(0.54078305, 0.039875678)^T$	$(0.00084279350, 0.00033244597)^T$
16	$(1.2195241, 0.10503114)^T$	$(0.0053202886, 0.0010113499)^T$
17	$(1.7953244, 0.13322287)^T$	$(0.0096274066, 0.00040332311)^T$
18	$(1.9952269, 0.037836236)^T$	$(0.00094441866, -0.0036342981)^T$
19	$(2.2766370, 0.10919590)^T$	$(-0.024969937, -0.10738732)^T$
20	$(2.5329448, 0.086488793)^T$	$(-0.067484112, -0.22341877)^T$
21	$(2.9324739, 0.19241566)^T$	$(-0.033494436, -0.48334012)^T$
22	$(0.0, 0.60)^T$	$(0.0030501201, 0.0014523155)^T$
23	$(0.5, 0.60)^T$	$(0.0046166793, 0.0025083792)^T$
24	$(1.0, 0.60)^T$	$(0.013060042, 0.0045300761)^T$
25	$(1.5, 0.60)^T$	$(0.033228801, 0.0072372634)^T$
26	$(2.0, 0.60)^T$	$(0.10004046, -0.020532766)^T$
27	$(2.5, 0.60)^T$	$(0.19505958, -0.20246448)^T$
28	$(3.0, 0.60)^T$	$(0.25710490, -0.53272069)^T$
29	$(3.5, 0.60)^T$	$(0.26893202, -0.92149933)^T$
30	$(4.0, 0.60)^T$	$(0.27413503, -1.3156280)^T$
31	$(0.0, 0.45)^T$	$(0.0031526205, 0.0014838105)^T$
32	$(4.0, 0.45)^T$	$(0.15685043, -1.3097350)^T$
33	$(0.0, 0.30)^T$	$(0.0025270661, 0.0013058087)^T$
34	$(4.0, 0.30)^T$	$(0.042305854, -1.3076245)^T$
35	$(0.0, 0.15)^T$	$(0.0014285077, 0.00090359659)^T$
36	$(4.0, 0.15)^T$	$(-0.71807578, -1.3068212)^T$
37	$(2.5, 0.00)^T$	$(-0.11364067, -0.20379047)^T$
38	$(3.0, 0.00)^T$	$(-0.17115245, -0.53300436)^T$
39	$(3.5, 0.00)^T$	$(-0.18317899, -0.92003269)^T$
40	$(4.0, 0.00)^T$	$(-0.18710608, -1.3067605)^T$

Table 2: The values of the 122 degrees of freedom at the steady MFE solution to the second example problem.